

10ème Congrès Français d'Acoustique

Lyon, 12-16 Avril 2010

Optimization of chaotic cavity transducers to nonlinear elastic imaging

Olivier Bou Matar¹, YiFeng Li¹, Steven Delrue², Koen Van Den Abeele²

¹ Joint European Laboratory LEMAC : Institut d'Électronique, de Microélectronique et de Nanotechnologie (IEMN - UMR CNRS 8520), Univ. Nord de France, ECLille, Cité Scientifique, BP48, 59651 Villeneuve d'Ascq, France

² K.U.Leuven Campus Kortrijk, E. Sabbelaan 53, B-8500 Kortrijk, Belgium

Recent results have shown that Nonlinear Elastic Wave Spectroscopy (NEWS) and Time Reversal (TR) techniques can be combined to precisely localize defects, produced by their nonlinear response. NEWS techniques can be used either as a post-treatment of TR used as a tool for ultrasound focusing in order to generate strong localized stress, or as a pre-treatment, of TR used as a tool for defect (nonlinear source) identification. Recently, it has been demonstrated that a single PZT ceramic glued on a chaotic cavity, a so called chaotic cavity transducer, can be used as a TR mirror or a multi-elements system on non reverberating samples. In this study, numerical and experimental results, performed in order to optimize the chaotic cavity transducer, and the time reversal process will be presented. The numerical results have been obtained with a nodal Discontinuous Galerkin Finite Element Method developed for the simulation of linear and nonlinear elastic wave propagation. The experimental set-up used is based on the combination of a chaotic cavity glued on the sample for the elastic wave emission (and focalization), and a laser vibrometer in order to image the nonlinear response at the surface of the sample. The obtained results enable us to find that chirp-coded excitation, instead of single-carrier short pulses, combined with inverse filter have to be used in order to transmit more energy per time on the defect, and so increase its nonlinear response, without increasing the peak intensity of the excitation. Moreover, the benefit of using emitters having a more or less chaotic shape is clearly found in breaking the symmetry of the problem, leading to an unambiguous retrofocusing.

1 Introduction

Recently, innovative ultrasonic methods have been developed to probe the existence of damage (e.g., delaminations, micro-cracks or weak adhesive bonds) by investigating various nonlinear signatures such as the generation of harmonics, the inter-modulation of frequency components, the amplitude dependent shift in resonance frequencies, the slow dynamic conditioning, etc [1]. Such approaches are termed Nonlinear Elastic Wave Spectroscopy (NEWS) techniques. The basis of all NEWS techniques is to measure and analyze macroscopic signatures resulting from a local violation of the linear stress-strain relation at the microscale [2]. Tests performed on a wide variety of materials subjected to different micro-damage mechanisms of mechanical, chemical and thermal origin, have shown that the sensitivity of such nonlinear methods to the detection of micro-scale features is far greater than what can be obtained with linear acoustical methods. NEWS methods have at first been applied for the global determination of the fatigue state of a structure, and recently extended to visualization techniques for imaging defect's nonlinearity distributions [3].

In the last five years, the concept of merging the benefits of both NEWS and Time Reversal Acoustic (TRA) has been proposed in order to realize images of defects in solid samples [4, 5]. In most NDT applications of this combination, a one channel TRA experiment has been used in which a piezoelectric (PZT) ceramic is glued directly to a sample. As demonstrated by Draeger *et al.* [6] in a silicon wafer chaotic cavity, the use of a one channel TRA system is possible because, in a cavity, multiple reflections tend to enhance the focusing quality both in resolution and in amplitude. As a consequence, the number of channels participating in the time reversal process can be reduced,

even to only one. This astonishing behavior has been linked to the ergodic property of the chaotic cavity, bearing the possibility to collect all information in only one point. Generally, the sample is small enough to be considered as multi-reverberant in the frequency range of interest [4, 5]. But, non-reverberant samples such as composite plates for instance are difficult to work with, and for systems with a high degree of symmetry, simple reverberating properties may lead to the concentration of virtual sources on a pattern with dimensions correlated to size of the sample (or the transducer) resulting in spatial diffraction figures and "phantom" images [5, 7]. In order to overcome the "phantom" image problem and to extend the method to non-reverberating sample, we have recently proposed to use a "chaotic cavity transducer" [8]. We have applied it for elastic waves in solids, and have demonstrated that a transducer glued on a chaotic cavity could be used as an array of transducers, as it was done for 3D imaging in fluid [9], but for imaging applications in solid medium, and more precisely to nonlinear imaging of defects such as cracks.

2 Chaotic Cavity Transducer

A "chaotic cavity transducer" consists of a combination of a PZT ceramic glued to a cavity of chaotic shape on the hardware side with the time reversal principle on the software side [8]. An applied source signal to the PZT ceramic generates a wave propagating in the cavity and the sample medium. Each time the propagating wave in the cavity arrives at the boundary between the cavity and the sample, part of the incident energy is reflected and continues to engender multiple reflections on the other boundaries of the cavity, whereas the other part of the energy is transmitted in the sample as shown on figure 1.

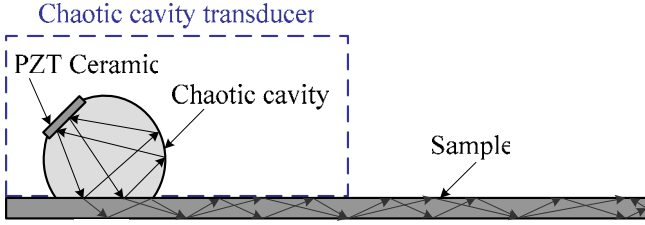


Figure 1: Principle of "chaotic cavity transducer".

2.1 Experimental Set-up

In the experiment discussed the setup shown on figure 2 has been used. A single PZT ceramic disk is glued to a chaotic cavity and, similarly, the cavity is glued onto the sample. The cavity made in copper has been designed in order to have the ergodic and mixing properties. A source signal, generated by an arbitrary wave generator coupled to a power amplifier, is applied to the PZT and generates travelling waves propagating in the cavity and radiating in the sample medium. In order to guarantee the synchronization of time reversal waves, the arbitrary wave generator AWG2021 is triggered by an external trigger generator. The out of plane velocity of the sample surface has been measured by a laser vibrometer. The signal is acquired through an oscilloscope LeCroy 9361. The reciprocal time reversal process and the scanning of the laser are computer controlled by Labview.

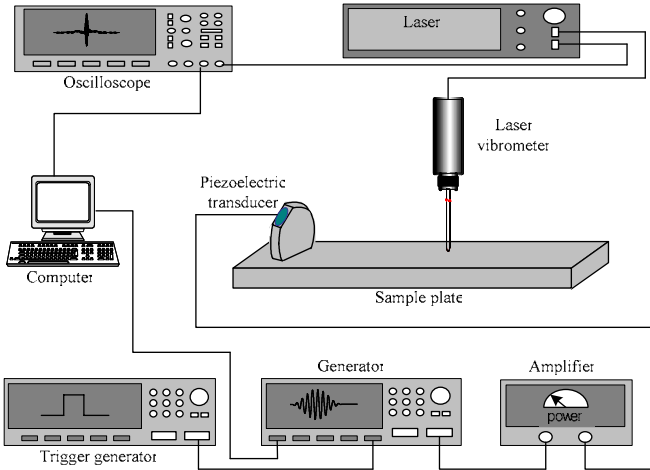


Figure 2: Experimental set-up used for the demonstration of the focusing properties of a "chaotic cavity transducer".

2.2 Signal Processing Methodology

Time Reversal (TR) provides the possibility to focus elastic waves in solid samples with only one channel when used in (or with) a multi-reverberant cavity. But, different kinds of signal processing methods can be used in order to improve both the Signal to Noise Ratio (SNR) and the quality of the focalization. In our study, two techniques have been tested: Chirped excitation and Inverse Filter.

Chirp Excitation

Experimentally, due to the low energy in the pulse, the use of a sinusoidal pulse signal for impulse response measurements does not provide a strong received signal, leading to a poor signal to noise ratio. So, for more robust measurement of the impulse response and to improve the quality of focalization a pulse compression technique with a

linear sweep signal has been used instead of the short sinusoidal pulse. Pulse compression is accomplished by taking the intercorrelation of the measured waveform with the time reversed input signal. There are three primary reasons why pulse compression is potentially a useful technique: to improve the available bandwidth of the imaging system, to detect the received signal even when it is well below the noise using cross-correlation techniques, and to transfer high energy levels into the test sample. This last reason is particularly interesting in nonlinear imaging of defect. Various types of swept-frequency signals have been proposed, as for example chirp signal, Barker and Golay codes, but it was found that the linear Frequency Modulated signal has the best performances in view of SNR improvement and robustness versus attenuation effects [10]. So, the pulse code we used is a chirp with linear increasing or decreasing instantaneous frequency:

$$s(t) = \cos(2\pi f_0 t + 2\pi \frac{B}{T} t^2), \quad -\frac{T}{2} \leq t \leq \frac{T}{2}, \quad (1)$$

where f_0 is the centre frequency, T is the signal duration and B is the total bandwidth that is swept. Comparison of the direct wave recorded signal and the retro-focalized signal obtained by using a sinusoidal pulse and a linear sweep source signal with the following parameters $T = 100 \mu s$, $f_1 = 200 \text{ kHz}$, $f_2 = 1000 \text{ kHz}$ ($B = f_2 - f_1$) are plotted on figure 3. It appears that the use of linear sweep source signal improves time recompression quality and signal to noise ratio.

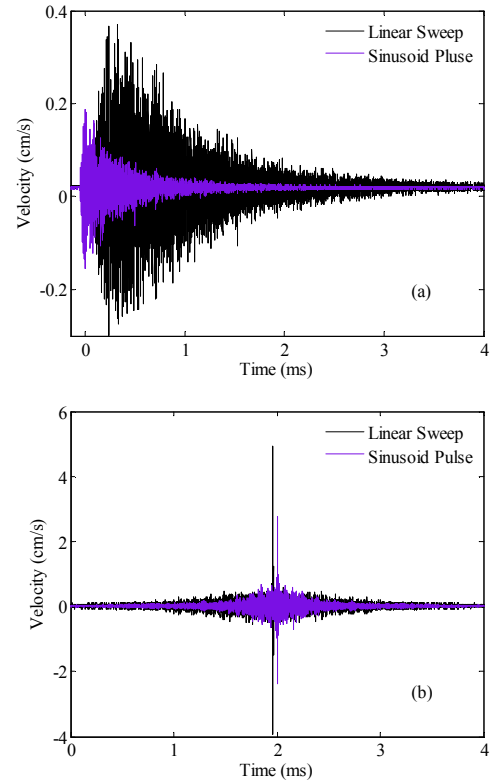


Figure 3: Comparison of (a) the direct wave recorded signal and (b) the time recompressed signal at the focus for two kinds of source signal: a sinusoidal pulse (purple line) and a linear sweep (black line).

Time Reversal and Inverse Filter

The spatio-temporal inverse filter was shown to improve the focusing quality [11]. Indeed, if linearity and spatial

reciprocity assumptions are valid in the medium, the preceding time reversal process corresponds to a spatial and temporal matched filter of the propagation. That is to say, the time reversal process maximizes the received output amplitude signal at a given location and a given time. The inverse filter allows calculation, both in space and time, of the set of temporal signals to be emitted in order to optimally focus on a chosen control point. Here, the Inverse Filter (IF) approach with a single transducer coupled to a chaotic and reverberant cavity consists in the inversion of the eigenmode energy [12]. The IF approach performs an inversion of the energy of the eigenmodes, and constructs the re-emitted signal as a linear combination of all the eigenmodes of the cavity, weighted by this inversion. Doing so, the focusing process takes advantage of all the modes including those with the weakest energy which are poorly exploited in the time reversal focusing process.

One of the more important parameters of the “chaotic cavity transducers” is the “signal-to-noise” contrast. As proposed by Quieffin [12], this contrast is the ratio between the energy of the signal at the recompression time $T_r = 0$ and the energy of the signal at all the others times. A physical interpretation of the contrast in terms of information grains has been given by Derode *et al.* [13]. In the case of a reverberating cavity, the information grains can be identified with the vibration eigenmodes of the cavity. Thus a contrast theory, for time reversal focusing in a cavity, can be developed using these vibration eigenmode formalism. Several physical parameters should be taken into account in this formalism: the absorption time τ_a of the material describing the damping of the impulse response, the Heisenberg time T_H of the cavity which could be viewed as the modal density of the cavity, that is to say the number of eigenmodes per frequency unit, and which depends on the volume of the cavity, the emission signal duration of the time reversed window ΔT , and the statistic of the distribution of the eigenmode amplitudes α and the frequency bandwidth $\Delta\Omega$. From the result obtained by Quieffin [12] three asymptotic behaviours can be considered. First, when the duration of the time reversed window ΔT is less than the Heisenberg time and the attenuation time, the contrast becomes proportional to the duration time and to the frequency bandwidth:

$$C = 4\sqrt{\pi} \Delta\Omega \Delta T, \quad (2)$$

In this case, the contrast linearly increases with the duration ΔT . In the second situation, the Heisenberg time is less than the duration ΔT and the attenuation time. In this case, the contrast becomes proportional to the Heisenberg time:

$$C = 4\sqrt{\pi} \Delta\Omega T_H \frac{\langle \alpha^2 \rangle^2}{\langle \alpha^4 \rangle}, \quad (3)$$

The third situation corresponds to the case where the attenuation time is shorter than both the Heisenberg time and the duration ΔT . The contrast becomes then proportional to the attenuation time:

$$C = 4\sqrt{\pi} \Delta\Omega \tau_a, \quad (4)$$

Figure 4 shows an example of the contrast, measured in the case of the copper chaotic cavity glued on a $12 \times 2.5 \times 1.0$ cm rectangular steel sample, as a function of the duration ΔT of the time reversed or inverse filtered signal.

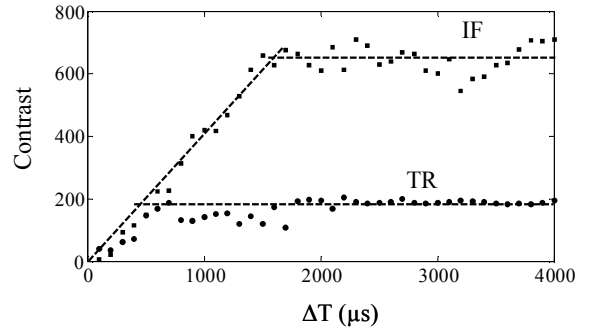


Figure 4: Contrast of the retro-focalised signal for Time Reversal (TR) and Inverse Filter (IF) processes.

An improvement by a factor of three can be observed using the IF technique. These properties are linked, as expected, to the fact that the number of eigenmodes used with IF method is higher than with TR (figure 5). The overall evolution of the contrast as a function of the duration of the time reversed window ΔT is in accordance with the theoretical description. When ΔT is less than the Heisenberg time T_H of the cavity and less than the characteristic attenuation time τ_a , the contrast linearly increases with ΔT . When ΔT is increased and becomes larger than T_H or τ_a , a saturation of the contrast appears. As a matter of fact, as the vibration eigenmodes represent the only frequencies present in the cavity, and as the frequency bandwidth is limited by the transducer that is used, the number of vibration eigenmodes of the cavity is limited as well, and consequently the contrast saturates. To understand which is the limiting factor between T_H and τ_a , an estimate of both of these time needs to be calculated. Unfortunately, as the chaotic cavity is glued on the sample, the measured absorption is not the main cause of decrease of the energy inside the cavity. Indeed, we want that a non negligible part of the energy propagates in the sample. In this case, the attenuation time τ_a of the cavity depends on the sample material. So, only an estimate of the Heisenberg time is accessible. Using a Weyl type formula [14] for the considered copper cavity, with a volume of 2.8 cm^3 and a surface of 6.22 cm^2 , the estimated Heisenberg time T_H is 10 ms, which is 10 times larger than the duration of the measured reverberating signal. So, the attenuation, mainly due to the radiation losses of the sample, appears to be the limiting factor, and for large values of ΔT the contrast simply becomes proportional to τ_a .

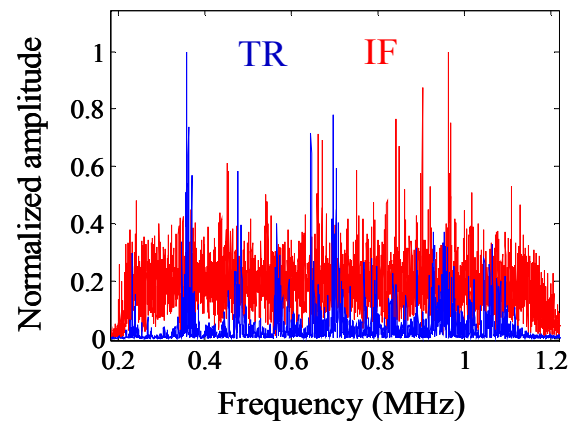


Figure 5: Comparison of the spectra of the time-recompression signal obtained with TR and IF methods.

3 Use of a chaotic cavity transducer on a Reverberant Medium

3.1 Experimental Results

In this part, experimental results obtained with TR or IF methods will be presented. In all the experiments, a linear sweep source signal has been used with the following parameters: $T = 100 \mu\text{s}$, $f_1 = 200 \text{ kHz}$, and $f_2 = 1200 \text{ kHz}$. First, an experiment for chaotic cavity transducer on a $12 \times 2.5 \times 1.0 \text{ cm}$ rectangular steel sample, using TR method, has been performed. In the first step, the focalization procedure presented in part 2 is used to retro-focalize on the chosen position on the surface of the sample. Then a 2D scan of $15 \times 15 \text{ mm}^2$, with a spatial step of 0.30 mm , of the wave field around the focal spot is made. Figure 6 displays snapshots of the wave field at the surface of the sample around the focus point at $T_r = -4 \mu\text{s}$, $-2 \mu\text{s}$, $0 \mu\text{s}$, $2 \mu\text{s}$ and $4 \mu\text{s}$. $T_r = 0$ corresponds to the instant of time recompression. These snapshots clearly show that the focusing wave comes from all around the focus point. This is due to the fact that, here, as the sample is multi-reverberant, it contributes to the retro-focusing process. Secondly, the same experiment, with the IF method in place of the TR, has been made. Figure 7 shows the process of the focalization at the same moment of time. Here, contrary to what Quieffin [12] have obtained in water with a chaotic cavity, the focal spot size is not decreased by the use of IF technique. Indeed, in both experiments the same 2 mm focal spot radius has been obtained, and is an estimate of the correlation length of the scattered wave field. Nevertheless, when one compares figures 6 and 7, the obtained contrast and time recompression clearly appear to have been improved by the use of the IF method. Moreover, the spatial distributions of the focused signal show no increase of the strain at the stress free boundary.

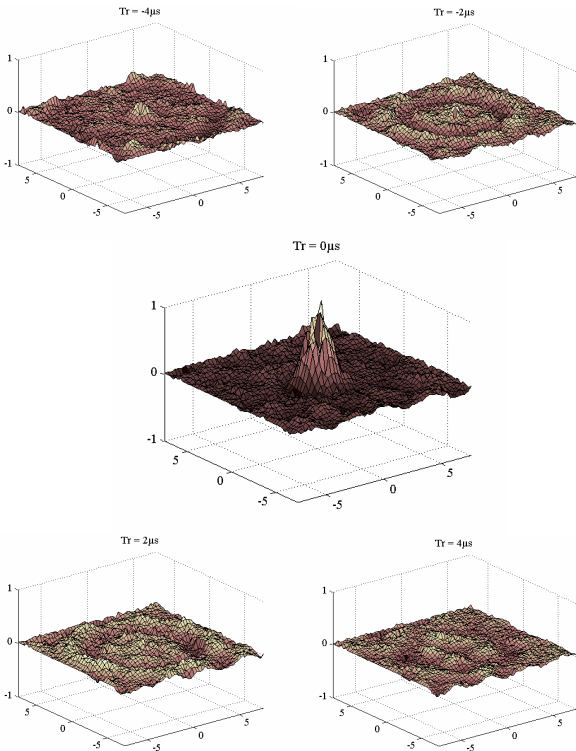


Figure 6: Snapshots of the surface particle velocity around the focal point at different moments of time showing the TR focalization obtained with a “chaotic cavity transducer”.

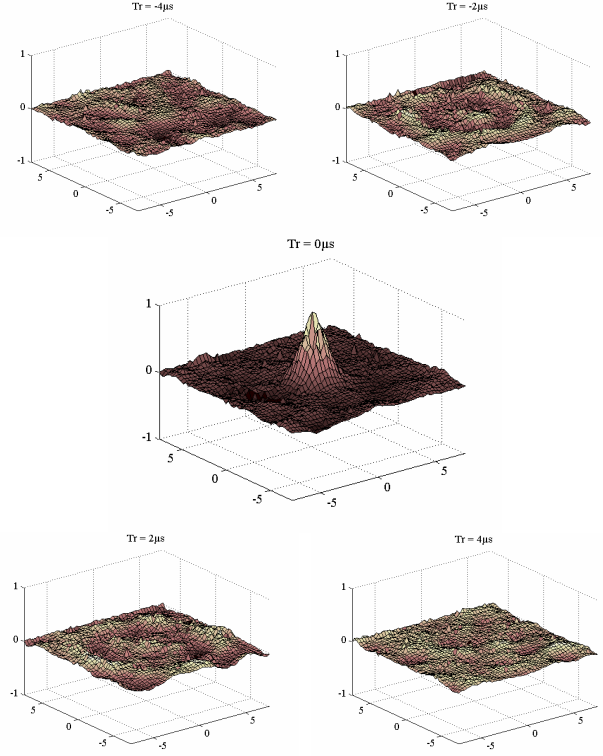


Figure 7: Snapshots of the surface particle velocity around the focal point at different moments of time showing the IF focalization obtained with a “chaotic cavity transducer”.

3.2 Simulation results

To give a better understanding of the “chaotic cavity transducer” concept, a numerical simulation study has also been made with a DG-FEM scheme [16]. The form and size of the chaotic cavity simulated is displayed in figure 8(a). It corresponds to a 2D version of the cavity used in the experiments. The source signal is a Ricker wavelet with a central frequency $f_c = 800 \text{ kHz}$ and is located in the middle of the tilted upper side border. The cavity material used in the experiments is copper with stress-free boundary condition on all the cavity boundaries. The following parameters have been used: $\rho_0 = 8930 \text{ kg/m}^3$, $C_{11} = C_{22} = 224.1 \text{ GPa}$, $C_{12} = 132.1 \text{ GPa}$ and $C_{66} = 46.0 \text{ GPa}$. The chosen point of focalization is positioned at $(0, -5) \text{ mm}$. The calculated received particle velocity signal at the focal point corresponds to a long-lasting reverberant signal. The total simulation time is $150 \mu\text{s}$ for this first step of the retro-focalization procedure. Then, a time reversed version of this signal is reemitted by a source located as before in the middle of the tilted upper side border. We can see, on the snapshot of the particle velocity at the moment of time recompression (figure 8(a)), that the spatial focalization point is at the position where the direct signal was received. The chaotic behaviour of the designed cavity seems to be adequate as no “phantom” image can be seen. The retro-focalized signal, calculated at the focal position, is displayed on figure 8(b). It confirms that the time recompression and correlation noise are inherent to the one channel time reversal process as in this numerical experiment this noise cannot be attributed to “thermal noise” or experimental errors. Now, the copper chaotic cavity is considered to be glued on a $27 \times 6 \text{ mm}$ reverberating steel plate: $\rho_0 = 7870 \text{ kg/m}^3$, $C_{11} = C_{22} = 237 \text{ GPa}$, $C_{12} = 141 \text{ GPa}$ and $C_{66} = 116 \text{ GPa}$. The same retro-focusing process is simulated but with the focusing point

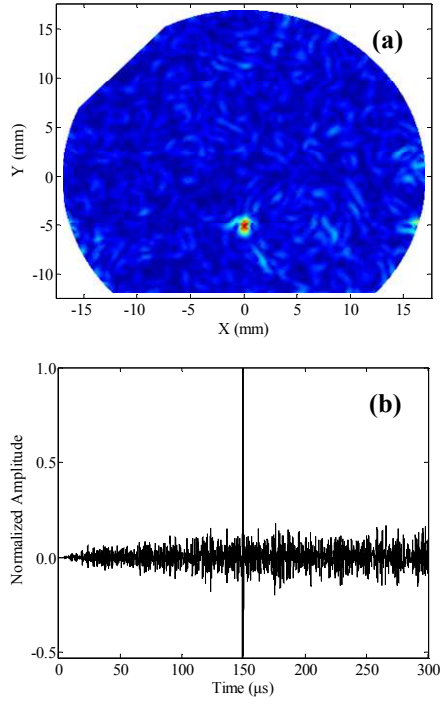


Figure 8: (a) Snapshot of the particle velocity at the moment of time recompression, (b) retro-focalized signal calculated for a copper chaotic cavity.

chosen in the steel plate at a position with coordinates (0,-8) mm. The obtained snapshot of the particle velocity at the moment of time recompression, figure 9(a), demonstrates the possibility of focusing in a sample with a one channel TR method combined with a chaotic cavity. It is to be noted that in this case the reflection at the interface between the cavity and the steel plate is rather small because their constituting materials are very similar. To see the influence of a higher impedance mismatch between the cavity and the

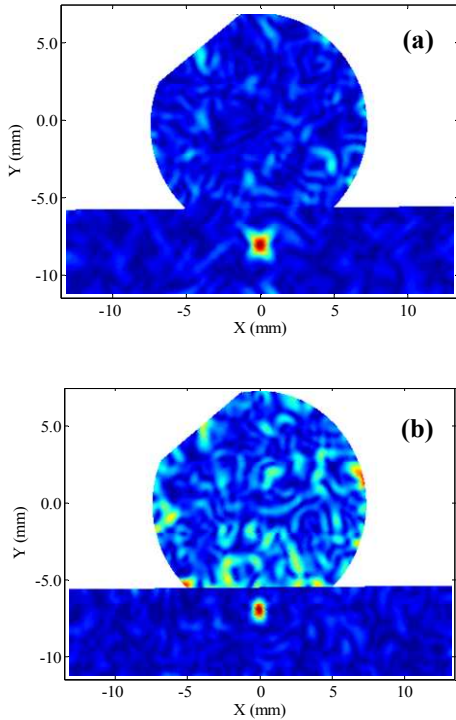


Figure 9: Snapshot of the particle velocity at the moment of time recompression calculated for a copper chaotic cavity glued on (a) a reverberating steel plate and (b) a composite plate of finite size.

sample on the retro-focusing process, we consider the case where the cavity is glued on a composite plate with the following material parameters: $\rho_0 = 1400 \text{ kg/m}^3$, $C_{11} = 20.28 \text{ GPa}$, $C_{22} = 20.52 \text{ GPa}$, $C_{12} = 5.59 \text{ GPa}$ and $C_{66} = 5.87 \text{ GPa}$. In this simulation, the receiver is located at the point (0.0,-7.0) mm. With the same procedure as in the two preceding calculations, we obtain the results plotted on figure 9(b), showing that it is possible to get a retro-focalization even on this medium with a high impedance mismatch.

4 Use of a chaotic cavity transducer on a Non-Reverberant Medium

The combination of single channel TR with non-reverberant samples poses serious problems for the technique as the sample cannot be used as a chaotic cavity. In this case, the use of the “chaotic cavity transducer” can be a solution to extend the possibility to focus in such sample with a one channel TR system. The same experiments as the one done in the preceding subsection for multi-reverberating steel sample will be repeated for a 2 mm thick non-reverberant composite plate of large dimension (30×20×0.2 cm). A 1×2×12 cm chaotic cavity glued on the composite plate was used. The chaotic behavior of the rectangular cavity used is induced by holes randomly made in it. The 2 cm width edge is the emitting edge of the “chaotic cavity transducer”. As in the reverberant sample experiments, a sweep of 100 μs duration and $f_{\min} = 200 \text{ kHz}$ and $f_{\max} = 1.2 \text{ MHz}$ combined with an inverse filter technique enables the focalization of elastic wave everywhere in the sample. The 2D scan of the amplitude of the wave field around the chosen focal spot, on a square of 15×15 mm² with a spatial step of 0.30 mm, is plotted on figure 10. This figure demonstrates that the “chaotic cavity transducer” works also on non-reverberating samples, even if the focalization quality is not as good as in the case of a reverberating sample. Here, as the sample is highly attenuating in the frequency range used, 200 kHz to 1.2 MHz, the surface particle velocity is quite small and difficult to measure with the laser vibrometer. As described in [8] the process of retro-focalization in this case is different from the one obtained previously with the reverberant sample. Indeed, here, the wave does not come from all around the focal point, but seems to propagate from the cavity. In fact, the behavior of the “chaotic cavity transducer” is now similar to the one we would obtain with a multi-elements transducer. The width of the focalization area should be

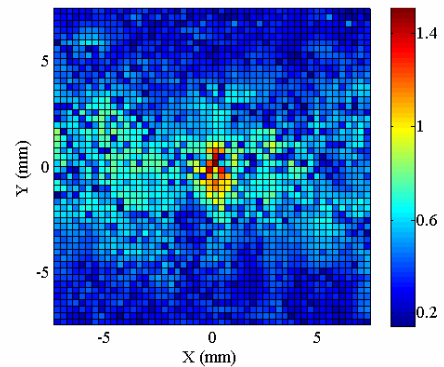


Figure 10: Experimental 2D scan of maximum amplitude measured during the retro-focalization process with the cavity 1×2×12 cm on a non-reverberant composite plate.

expressed as $\Delta R = \lambda F/D$, where D is the width of the chaotic cavity in the direction of focalization, F the focal distance, and λ the wavelength of the dominant transmitted mode. To simulate a non-reverberating sample a NPML absorbing layer [16] is used to be able to consider the sample as a semi infinite medium. Snapshots of the particle velocity at five instants around the time recompression are displayed on figure 11. One can clearly see that the wave does not come from all around the focal point as in the case where the “chaotic cavity transducer” is glued on a reverberant sample, but propagates from the cavity. A point, which can not be measured experimentally, is the fact that in the considered case, where the sample presents a high impedance mismatch with the cavity, the focusing properties is mainly linked to surface waves propagating at the interface between the cavity and the sample. Finally, careful look at the snapshots brings to light a “phantom” focal point, inside the cavity.

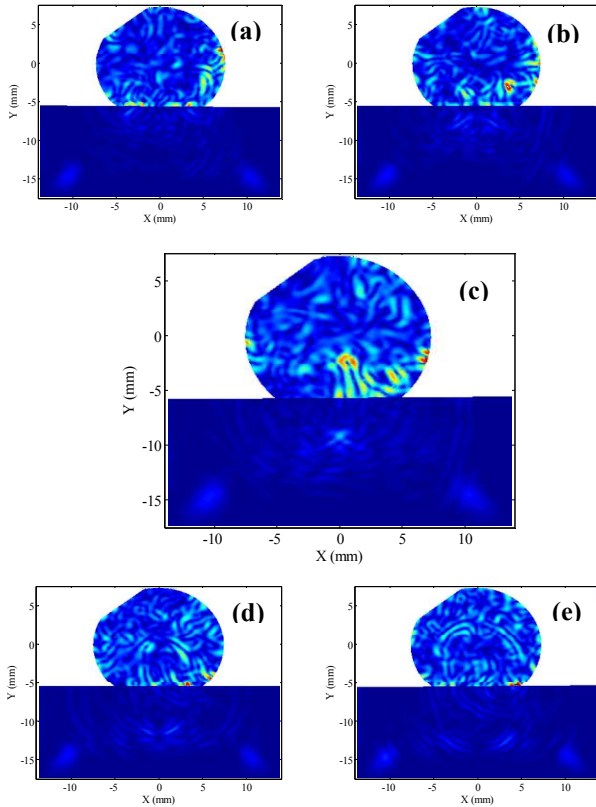


Figure 11: Calculated snapshots of the particle velocity at (a) $t = 97.3 \mu s$, (b) $t = 98.3 \mu s$, (c) $t = 99.2 \mu s$, (d) $t = 100.4 \mu s$, and (e) $t = 101.4 \mu s$ for a copper chaotic cavity glued on a non reverberating composite sample.

5 Conclusion

An experimental and numerical study of the use of the concept of “chaotic cavity transducer” to focalize in reverberant and non-reverberant solid media with only one source has been made. The main advantages of using chaotic cavities that have been demonstrated both numerically and experimentally are the elimination of phantom images and boundary effects in the retro-focalization process, and the offered possibility to focus energy in non-reverberating samples. In this case, the sample does not contribute to the focusing process and the focusing is achieved by propagating wave that solely come from the direction of the transducer and not from every direction around the focal spot, contrary to what is obtained in a reverberant sample.

Références

- [1] Van Den Abeele K., Sutin A., Carmeliet J., Johnson P.A., "Microdamage diagnostics using nonlinear elastic wave spectroscopy (NEWS)," *NDT & E Int.* 34, 239–248 (2001).
- [2] Guyer R.A., Johnson P.A., "Nonlinear mesoscopic elasticity: Evidence for a new class of material," *Phys. Today* 52, 30-36 (1999).
- [3] Solodov I., Wackerl J., Pfeleiderer K., Busse G., "Nonlinear self-modulation and subharmonic acoustic spectroscopy for damage detection and location," *Appl. Phys. Lett.* 84, 5386-5388 (2004).
- [4] Sutin A., TenCate J.A., Johnson P.A., "Single-channel time reversal in elastic solids," *J. Acoust. Soc. Am.* 116, 2779-2784 (2004).
- [5] Ulrich T.J., Johnson P.A., Guyer R., "Interaction Dynamics of Elastic Waves with a Complex Nonlinear Scatterer through the Use of a Time Reversal Mirror," *Phys. Rev. Lett.* 98, 104301 (2007).
- [6] Draeger C., Fink M., "One-Channel Time Reversal of Elastic Waves in a Chaotic 2D-Silicon Cavity," *Phys. Rev. Lett.* 79 (3), 407-410 (1997).
- [7] Goursolle T., Calle S., Dos Santos S., Bou Matar O., "A two-dimensional pseudospectral model for time reversal and nonlinear elastic wave spectroscopy," *J. Acoust. Soc. Am.* 122 (6), 3220–3229 (2007).
- [8] Bou Matar O., Li Y.F., Van Den Abeele K., "On the use of a chaotic cavity transducer in nonlinear elastic imaging," *Appl. Phys. Lett.* 95, 141913 (2009).
- [9] Montaldo G., Palacio D., Tanter M., Fink M., "Time reversal kaleidoscope: A smart transducer for three-dimensional ultrasonic imaging," *Appl. Phys. Lett.* 84 (19), 3879-3881 (2004).
- [10] Misaridis T., Jensen J.A., "Use of modulated excitation signals in medical ultrasound. Part I. Basic concepts and expected benefits," *IEEE Trans. Ultrason, Ferroelect, Freq. Contr.* 52 (2), 177-191 (2005).
- [11] Tanter M., Thomas J.L., Fink M., "Time reversal and the inverse filter," *J. Acoust. Soc. Am.* 108, 223-234 (2000).
- [12] Quieffin N., "Etude du rayonnement acoustique de structures solides : vers un système d'imagerie haute résolution," Thèse de Doctorat de l'Université Paris VI (2004).
- [13] Derode A., Tourin A., Fink M., "Ultrasonic pulse compression with one bit time reversal through multiple scattering," *J. App. Phys.* 85 (9), 6343-6352 (1999).
- [14] Weaver R. L., "On diffuse waves in solid media," *J. Acoust. Soc. Am.* 71 (6), 1608-1609 (1982).
- [16] Bou Matar O., Li Y.F., Preobrazhensky V., Pernod P., "Une méthode Galerkin Discontinue nodale pour la propagation non linéaire d'ondes élastiques" in these proceedings.